# Some more on Gamma-Astronomy: Why on satellites?

Atmosphere:

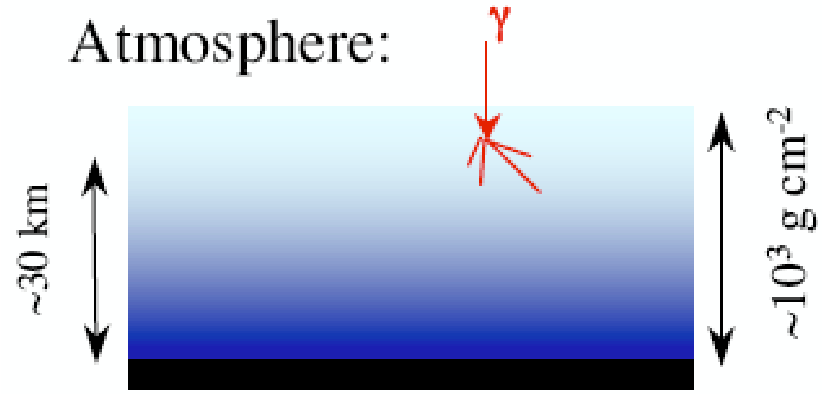


For $E_\gamma$ < ~ 100 GeV, must detect above atmosphere (balloons, satellites)

For $E_\gamma$ > ~100 GeV, information from showers penetrates to the ground (Cerenkov, air showers)

# Summary of techniques

- **Space-based:**
  - use pair-conversion technique

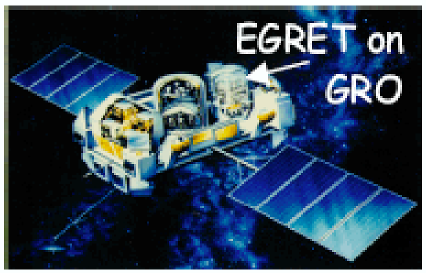


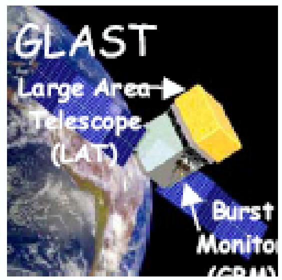


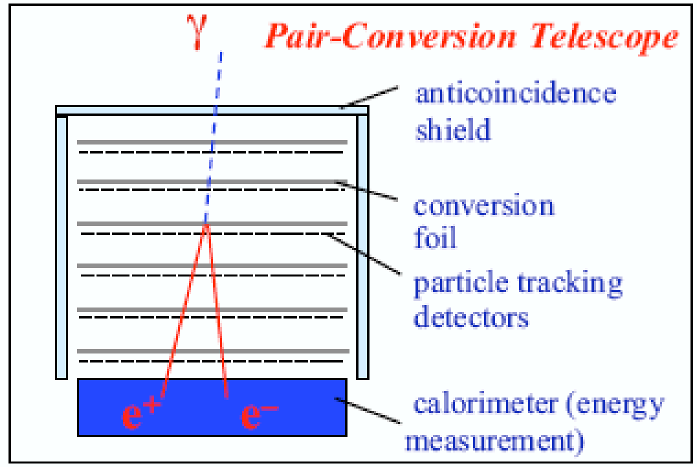


- **Ground-Based:**
  - Airshower Cerenkov Telescopes (ACTs)

image the Cerenkov light from showers induced in the atmosphere. Examples: Whipple, STACEE, CELESTE, VERITAS

  - Extensive Air Shower Arrays (EAS)

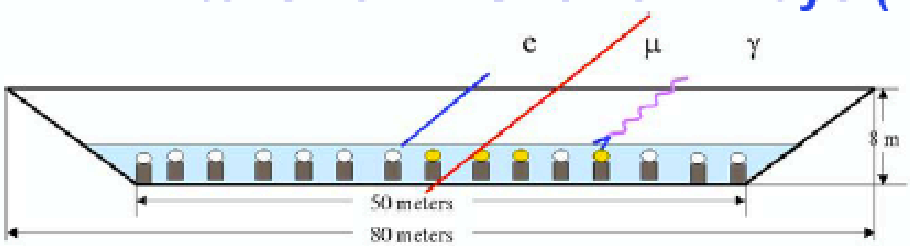


Directly detect particles from the showers induced in the atmosphere. Example: MILAGRO

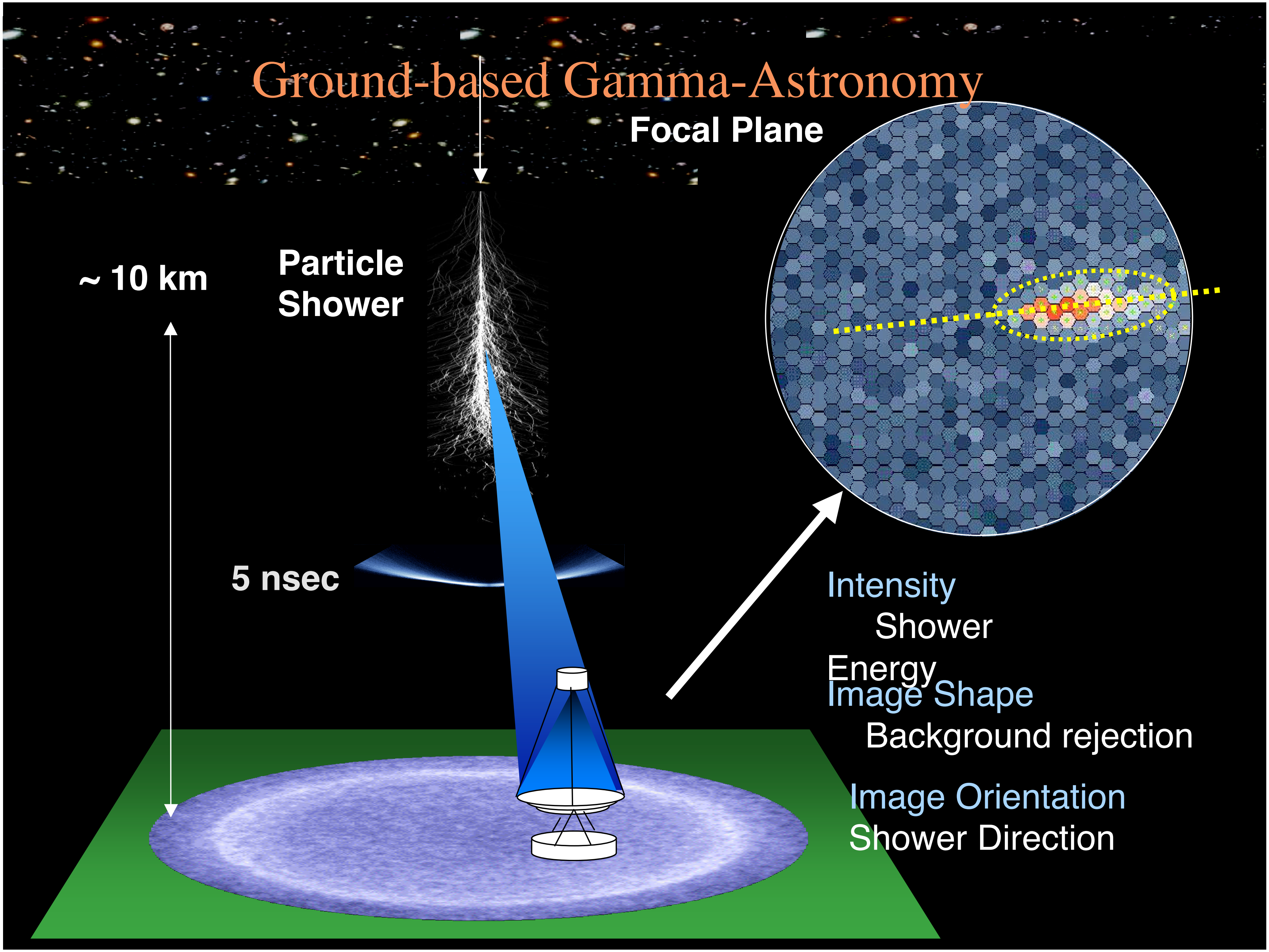
Ground-based Gamma-Astronomy
Focal Plane
Particle Shower
~ 10 km
5 nsec
Intensity
Shower Energy
Image Shape
Background rejection
Image Orientation
Shower Direction

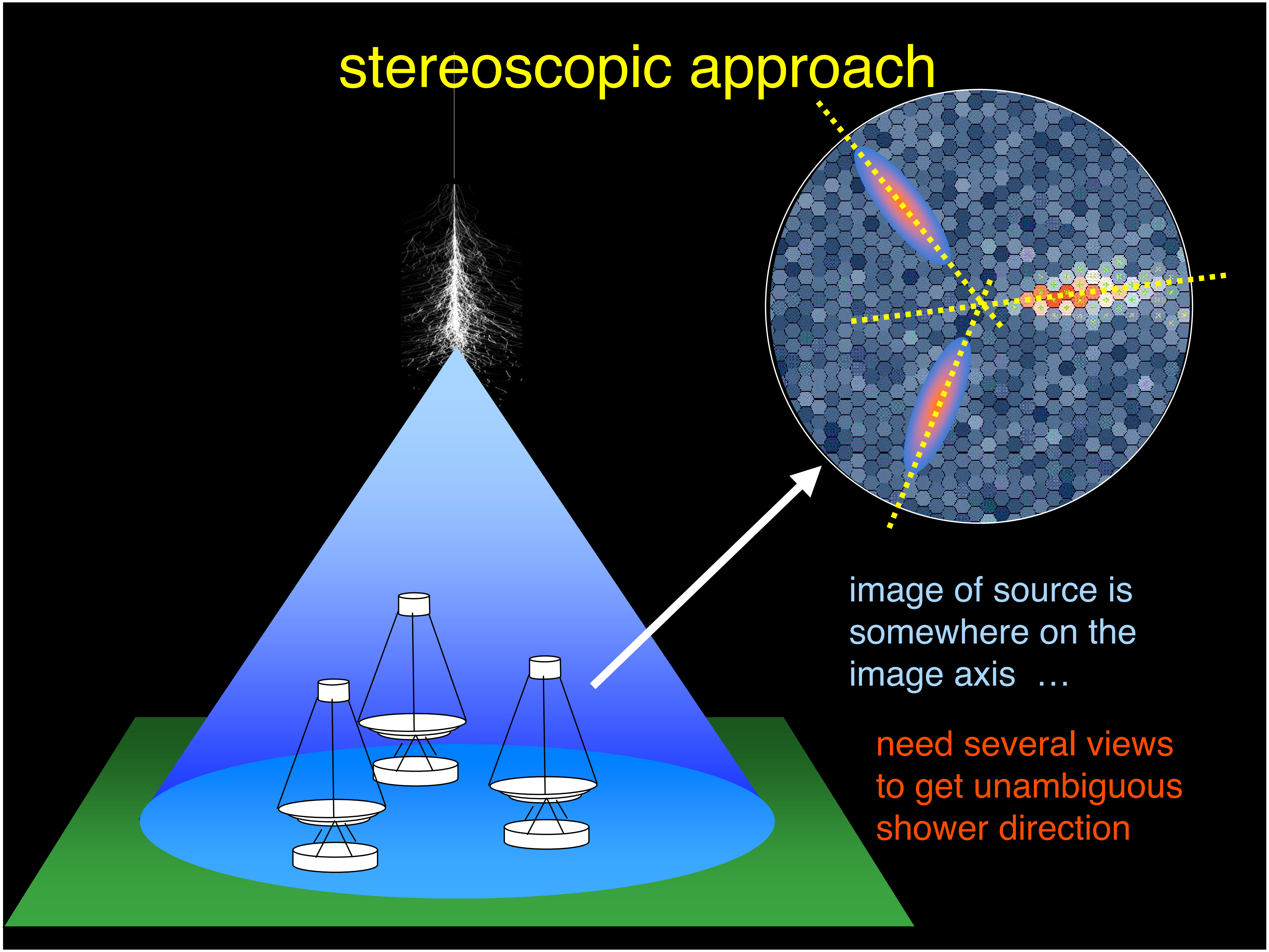
stereoscopic approach
image of source is somewhere on the image axis …
need several views to get unambiguous shower direction

# Attenuation of photons

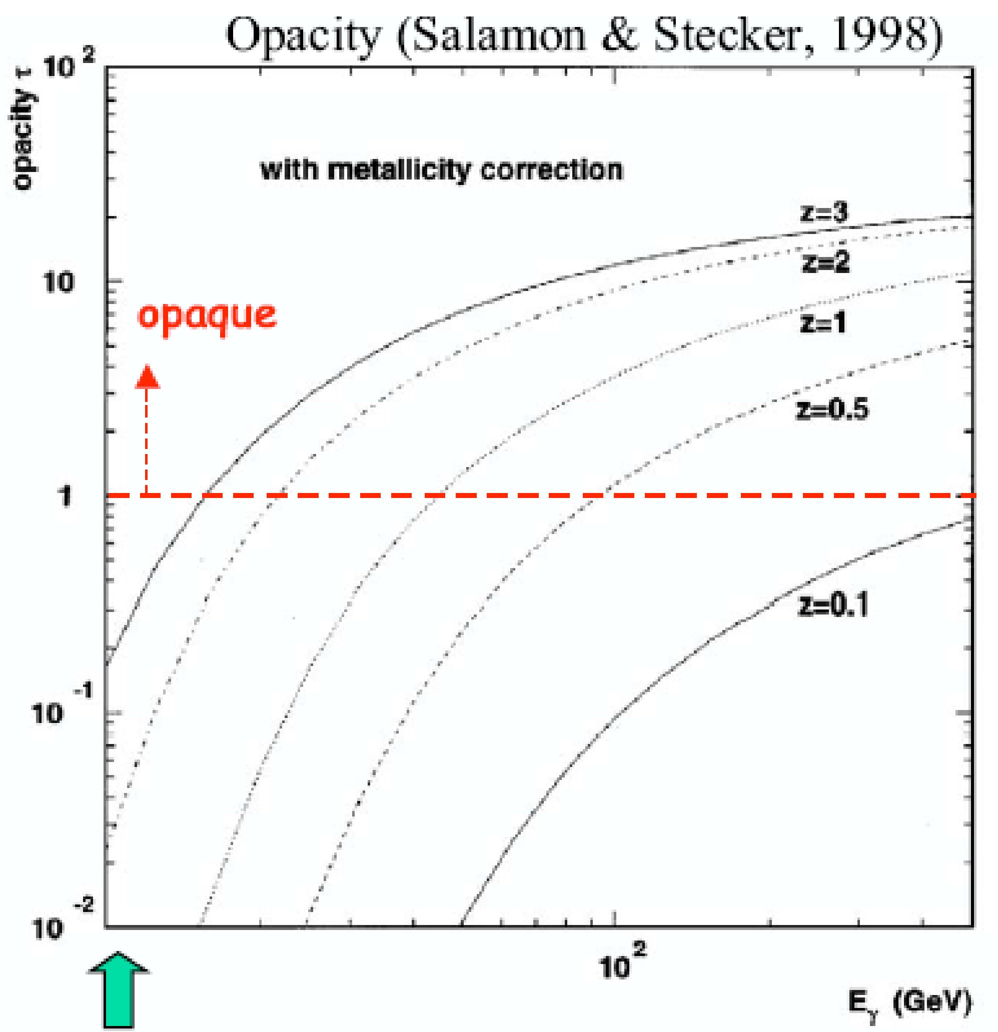


No significant attenuation below ~10 GeV.

- Photons with E> 10 GeV are attenuated by optical-IR extragalactic background light (EBL)
- Only $e^{-\tau}$ of the source flux reaches us
- Important investigation for GLAST

# The gamma-ray sky

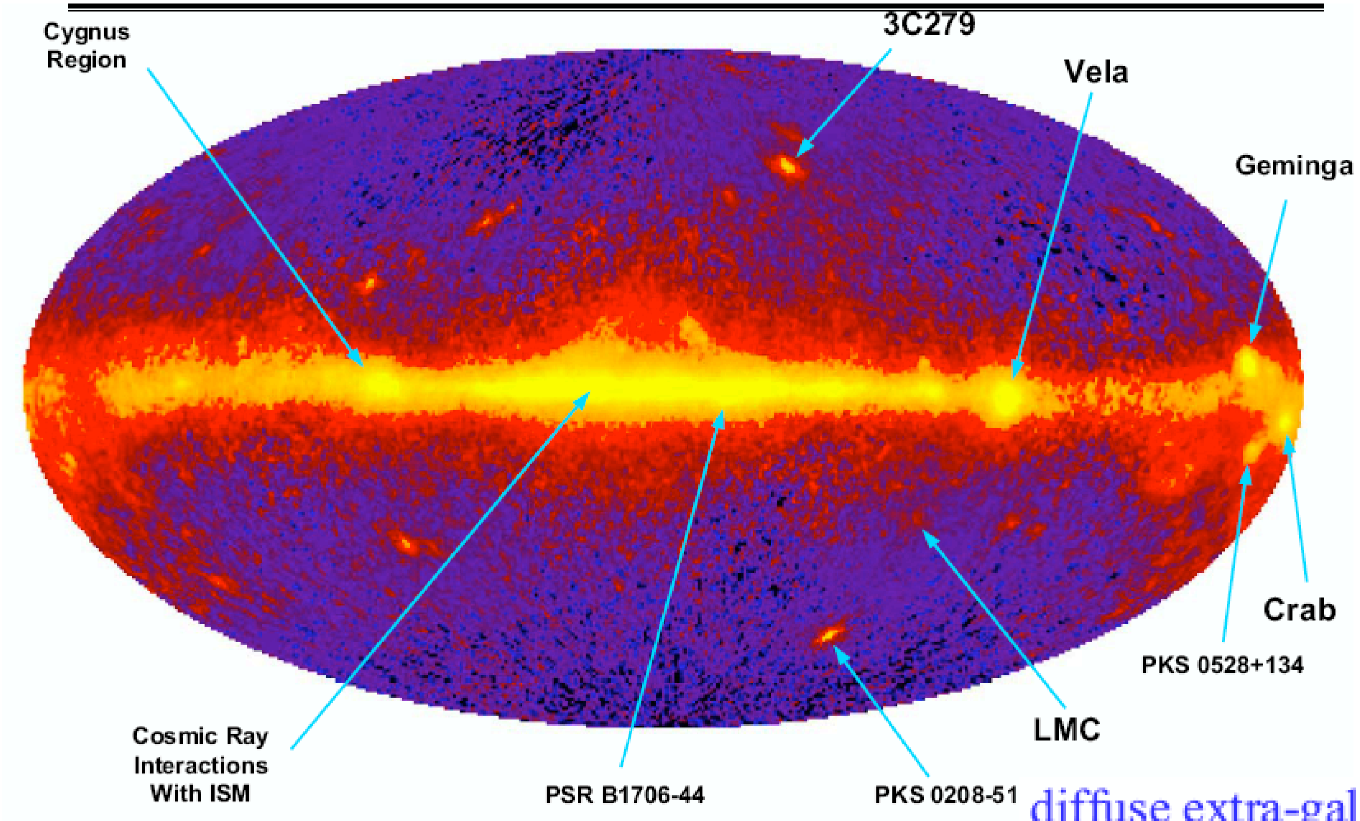


diffuse extra-galactic background
(flux ~ $1.5 \times 10^{-5}$ $cm^{-2}s^{-1}sr^{-1}$)

galactic diffuse (flux ~O(100) times larger)

high latitude (extra-galactic) point sources (typical flux from EGRET sources O($10^{-7}$ - $10^{-6}$) $cm^{-2}s^{-1}$

# The VHE Sky – today

**11 Galactic, 11 Extragalactic, GC, plus 15 unidentified**

**not many sources ... but at least 7 source populations !**

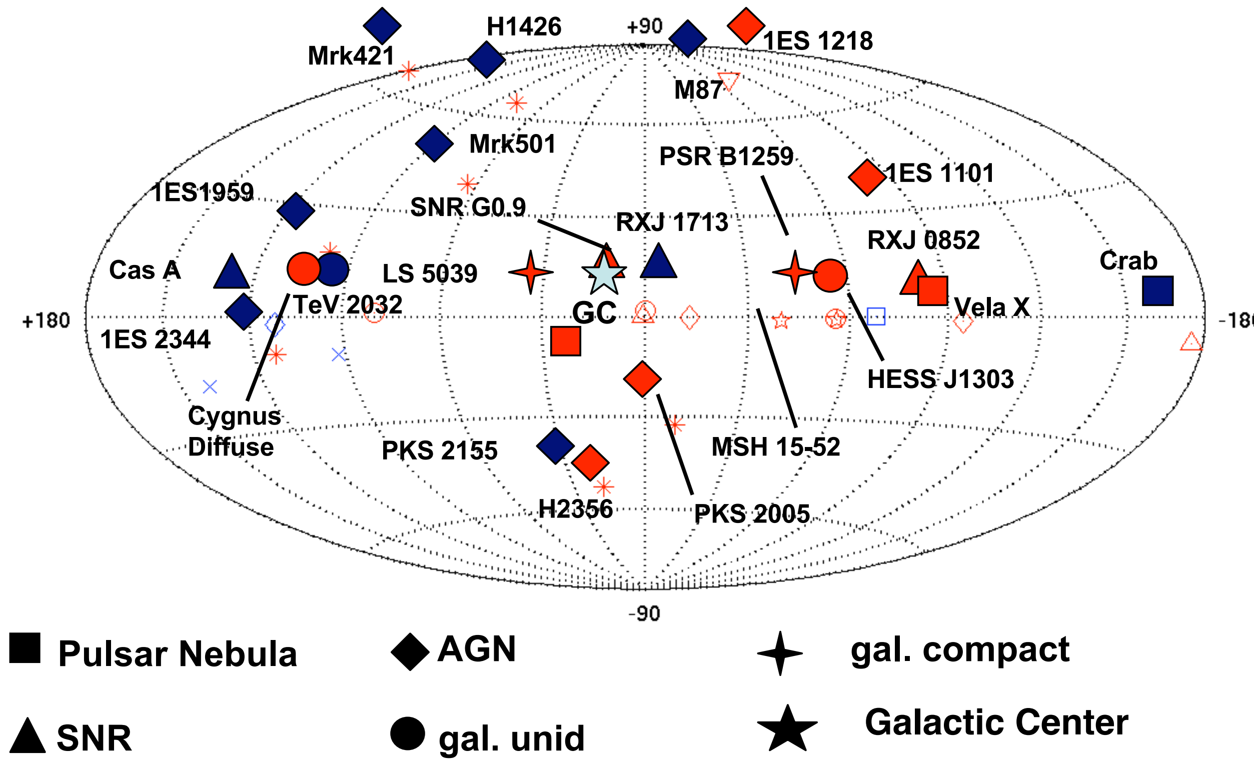

# H.E.S.S. survey of the central region of the Galactic Plane

## → 15 more (yet unidentified) sources

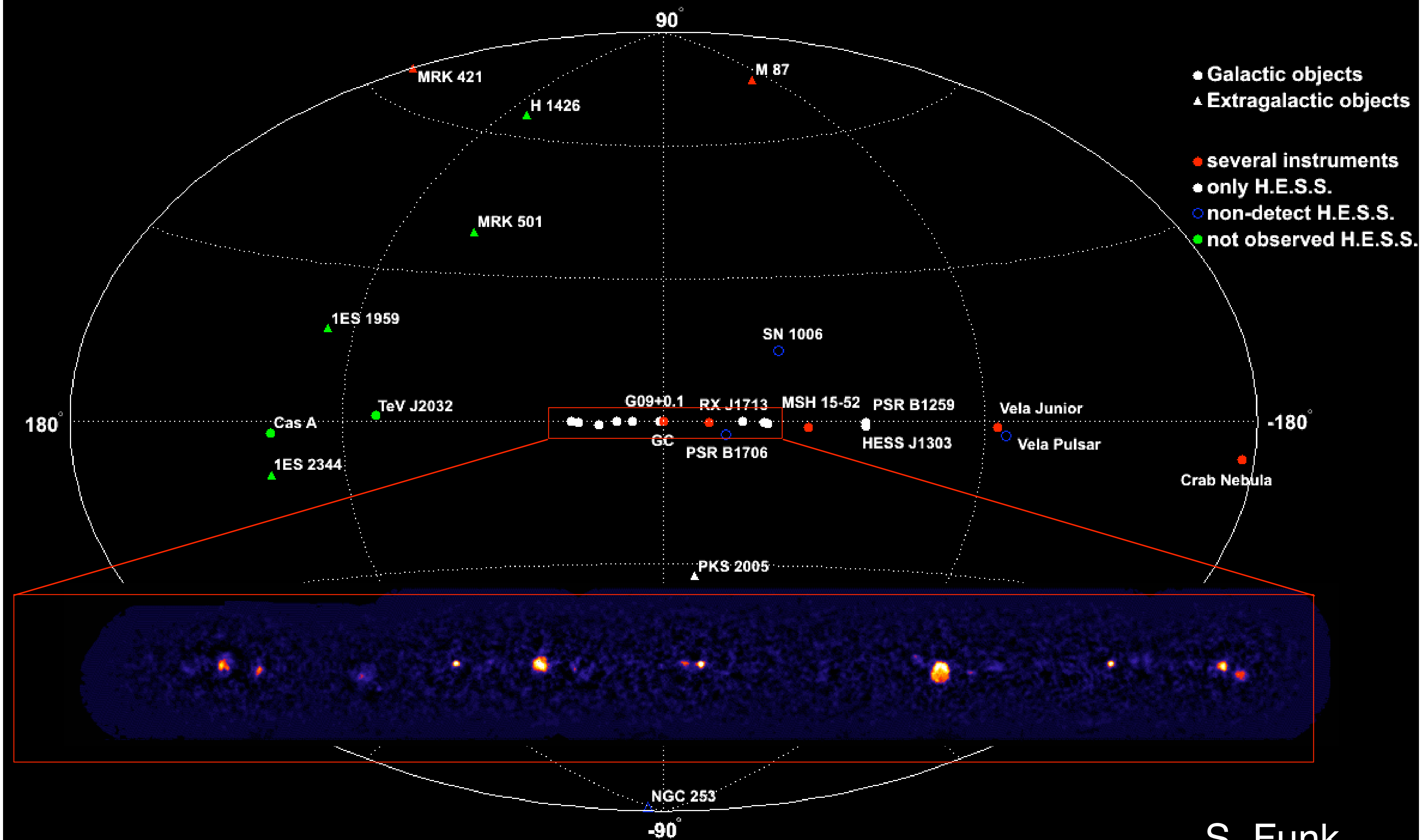


S. Funk

# http://www.icrr.u-tokyo.ac.jp/~morim/TeV-catalog.htm

TeV Source Catalog

| Name | RA | Decl | GL | GB | Claim | Comment | No. |
|---|---|---|---|---|---|---|---|
| NGC 253 | 11.888 | -25.2882 | 97.369 | -87.964 | C2, ~H | Starburst Gal., z=0.00080 | 1 |
| 3C66A | 35.66505 | 43.0355 | 140.143 | -16.767 | Cr | QSO, z=0.444 | 2 |
| PSR0531+21 | 83.63288 | 22.01446 | 184.557 | -5.785 | Many | Crab pulsar/nebula | 3 |
| PSR0833-45 | 128.8359 | -45.1766 | 263.552 | -2.787 | C1, ~H | Vela pulsar | 4 |
| RXJ0852.0-4622 | 132.2458 | -45.6333 | 265.385 | -1.181 | C2, H | SNR, G266.6-1.2, Vela Jr. | 5 |
| Mkn 421 | 166.1138 | 38.20883 | 179.832 | 65.031 | Many | XBL, z=0.031 | 6 |
| Cen X-3 | 170.3132 | -60.6233 | 292.09 | 0.336 | D | X-ray binary | 7 |
| M87 | 187.7059 | 12.39112 | 283.778 | 74.491 | H | Radio galaxy, z=0.00436 | 8 |
| PSR1259-63/SS2883 | 195.6987 | -63.8357 | 304.184 | -0.992 | H | PSR/Be binary | 9 |
| HESS J1303-631 | 195.7642 | -63.1986 | 304.241 | -0.356 | H | UnID | 10 |
| H1426+428 | 217.1354 | 42.67361 | 77.49 | 64.899 | Many | XBL, z=0.129 | 11 |
| SN1006 | 225.5919 | -41.8962 | 327.514 | 14.642 | C1, ~H | SNR, G327.6+14.6 | 12 |
| MSH15-52 | 228.5292 | -59.1575 | 320.330 | -1.192 | C1, H | SNR, G320.4-1.2, HESS J1514-591 | 13 |
| HESS J1614-518 | 243.5679 | -51.8442 | 331.497 | -0.594 | H | | 14 |
| HESS J1616-508 | 244.1033 | -50.8964 | 332.394 | -0.140 | H | PSR J1617-5055? | 15 |
| HESS J1640-465 | 250.1829 | -46.5319 | 338.317 | -0.021 | H | G338.3-0.0? | 16 |
| Mkn 501 | 253.4672 | 39.76004 | 63.6 | 38.859 | Many | XBL, z=0.034 | 17 |
| PSR1706-44 | 257.426 | -44.4825 | 343.1 | -2.683 | C1, ~H | 3EGJ1710-4439 | 18 |
| RXJ1713.7-3946 | 258.425 | -39.7667 | 347.346 | -0.498 | C1, C2, H | SNR, G347.3-0.5 | 19 |
| Sgr A* | 266.4169 | -29.0078 | 359.944 | -0.046 | C2, W, H | Gal.C.[Rogers et al.1994 ApJ434L59] | 20 |
| G0.9+0.1 | 266.8467 | -28.1517 | 0.872 | 0.076 | H | SNR | 21 |
| HESS J1804-216 | 271.1329 | -21.6919 | 8.408 | -0.027 | H | G8.7-0.1 / W30? | 22 |
| HESS J1813-178 | 273.4079 | -17.8428 | 12.813 | -0.034 | H | SNR AX J1813-178/AGPS273.4-17.8 | |
| HESS J1825-137 | 276.5150 | -13.7633 | 17.820 | -0.743 | H | G18.0-0.7 ? | 24 |
| HESS J1826-148 | 276.5626 | -14.8783 | 16.882 | -1.289 | H | LS 5039 | 25 |
| HESS J1834-087 | 278.7104 | -8.7533 | 23.258 | -0.329 | H | G23.3-0.3 / W41 ? | 26 |
| HESS J1837-069 | 279.4279 | -6.9275 | 25.206 | -0.121 | H | G25.5+0.0 ? | 27 |
| 1ES1959+650 | 299.9994 | 65.14852 | 98.003 | 17.67 | U, W, HC | XBL, z=0.048 | 28 |
| PKS2005-489 | 302.3721 | -48.8219 | 350.386 | -32.611 | H | XBL, z=0.071 | 29 |
| TeV J2032+4130 | 308.0292 | 41.50833 | 80.254 | 1.074 | HC | UnID: Cyg OB2? | 30 |
| PKS2155-304 | 329.7169 | -30.2256 | 17.73 | -52.246 | D, H | XBL, z=0.117 | 31 |
| Cas A | 350.8529 | 58.8154 | 111.736 | -2.13 | HC | SNR, G111.7-2.1 | 32 |
| BL Lac | 330.6807 | 42.27779 | 92.59 | -10.441 | Cr | z=0.0686 | 33 |
| 1ES2344+514 | 356.7702 | 51.70497 | 112.891 | -9.908 | W | XBL, z=0.044 | 34 |

Claim: W: Whipple, C1: CANGAROO-I, C2: CANGAROO-II, D: Durham, Cr: Crimea, HC: HEGRA CT, H: H.E.S.S., ~H: H.E.S.S. upper limit

# TeV $\gamma$ ray source populations

## Extended Galactic Objects

- Shell Type SNRs
- Giant Molecular Clouds (star formation regions)
- Pulsar Wind Nebulae plerions

## Compact Galactic Sources

- Binary pulsar PRB 1259-63
- LS5039 – a Microquasar

## Galactic Center

Review on Galactic sources Bednarek, Burgio, TM,
http://arxiv.org/pdf/astro-ph/0404534

## Extragalactic objects

- M87 - a radiogalaxy
- TeV Blazars – with redshift from 0.03 to 0.18

- and a large number of yet unidentified TeV sources …

# RXJ1713.7-3946 is a TeV source !

energy spectrum   and   morphology

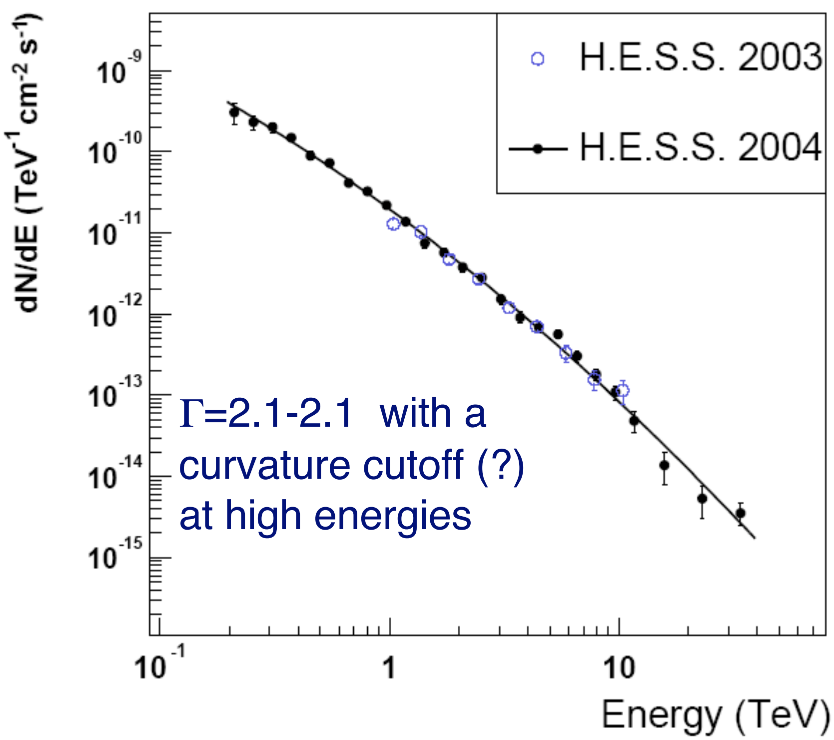


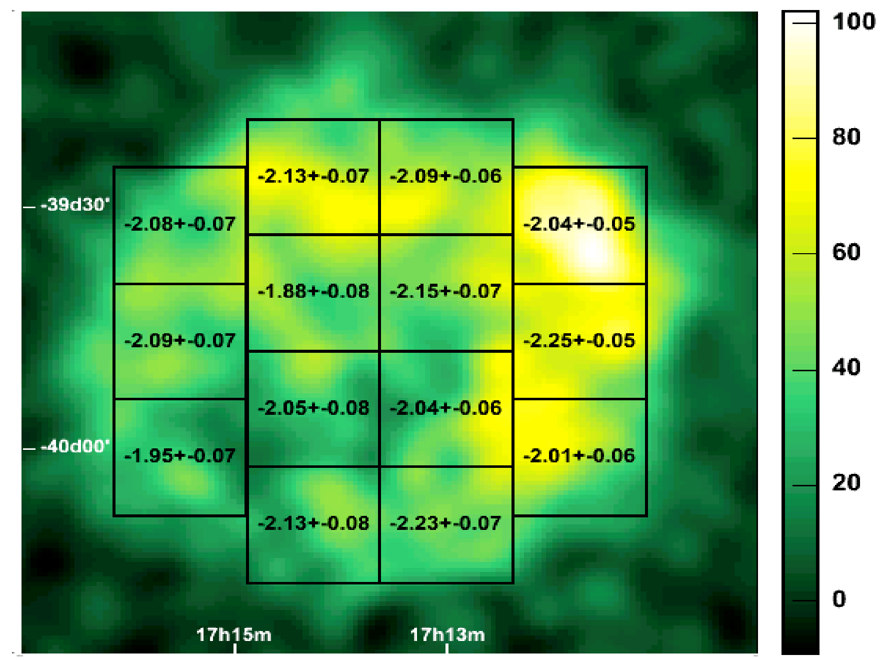


Γ=2.1-2.2 -evidence of acceleration of protons ?

no significant spectral variation

*if a coordinate-independent single power law*

*from* 100 GeV to 10 TeV

difficult to explain  by IC

# Vela Junior (a 2° diameter remnant)

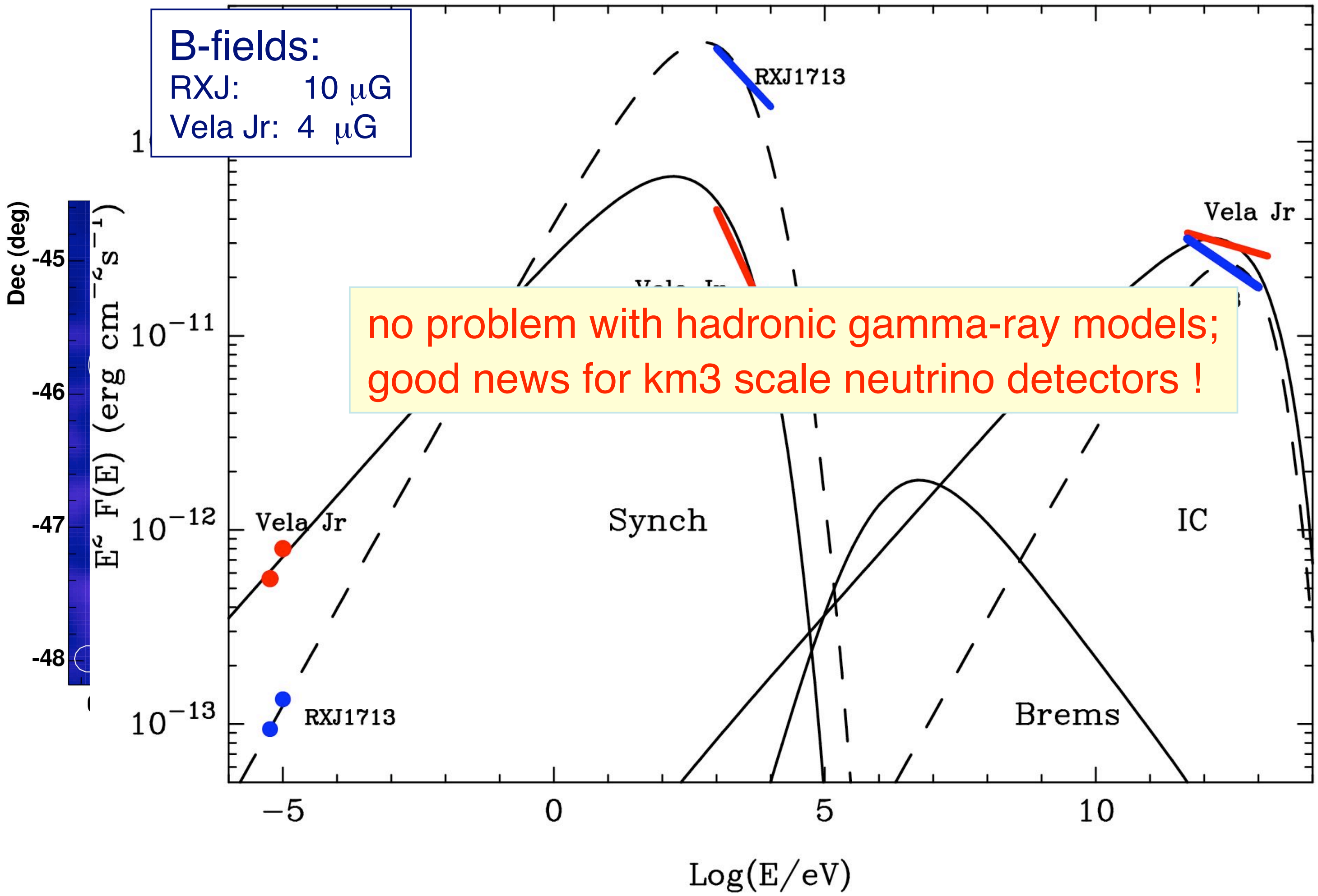


no problem with hadronic gamma-ray models;
good news for km3 scale neutrino detectors !

IC origin ? – very small B-field, $B < 10\ \mu G$, <u>and</u>

very large $E_{max} > 100$ TeV

two assumptions hardly can co-exists within standard acceleration models

# Crab unit

- This is a unit of X-ray intensity evaluated at 5.2 keV, or over a band pass from 2 - 11 keV. If an X-ray source has the same type of spectrum as the Crab Nebula between 2 - 11 keV, we can compare them according to their brightness in Crab units. Numerically, 1 Crab equals 1060 microJanskys, and 1 microJansky = 0.242 x 10^-11 ergs cm^-2 sec^-1 keV^-1 or 1.51 x 10^-3 keV cm^-2 sec^-1 keV^-1.

  Example, at 2-11 keV, the star Algol produces 9 microJanskys or 9/1060 = 0.0085 Crabs, assuming Algol's spectrum has the same shape as the Crab nebula between 2 - 11 keV.

- http://www.icrr.u-tokyo.ac.jp/~morim/CrabUnit.html

Ref: Crab flux: Aharonian et al., ApJ 614, 897 (2004)

[2.83E-11*(E/TeV)^(-2.62) /cm2 /s /TeV]

- SourceDiff. Index   2.62
- Energy threshold (GeV)  500
- Integral flux (Crab unit)

# HESS Catalogue

http://www.mpi-hd.mpg.de/hfm/HESS/public/HESS_catalog.htm

| Source identifier | Source coordinates (J2000) Ra | Dec | Flux (Crab units) | Size (arcmin) | Counterpart / other names | Reference |
|---|---|---|---|---|---|---|
| HESS J0852-463 | 8h52m | 46d20’ | ~100% | ~40 | **RX J0852-4622 (Vela Jr)** | A&A 437 (2005) L7 |
| HESS J1104-382 | 11h04m27.6s | 38d12' 54” | ~300% | not extended | **Mkn 421** | A&A 437 (2005) 95 |
| HESS J1302-638 | 13h02m49.3s | -63d49' 53'' | up to ~10% | not extended | **PSR B1259-63** | A&A 442 (2005) 1 |
| HESS J1303-631 | 13h03m0.4s | -63d11' 55'' | ~17% | ~10 | -- | A&A 439 (2005) 1013 |
| HESS J1514-591 | 15h14m7s | -59d9' 27'' | ~15% | ~6x2 | **MSH 15-52 / PSR B1509–58** | A&A 435 (2005) L17 |
| HESS J1614-518 | 16h14m19.0s | -51d49' 7'' | ~25% | ~12 | -- | Science307(2005)1938 * ApJ 636 (2006)777 |
| HESS J1616-508 | 16h16m23.6s | -50d53' 57'' | ~19% | ~8 | PSR J1617-5055 ? | Science307(2005)193 |
| HESS J1632-478 | 16h32m8.6s | -47d49' 24'' | ~12% | 8 | IGR J16320-4751, AX J163252-4746 ? | ApJ636(2006) 777 |
| HESS J1634-472 | 16h34m57.2s | -47d16' 2'' | ~6% | ~7 | IGR J16358-4726, G337.2+0.1 ? | ApJ 636 (2006) 777 |
| HESS J1640-465 | 16h40m44.2s | -46d31' 44'' | ~9% | ~2 | G338.3-0.0 ? 3EG J1639-4702 ? | Science307(2005) 193 |
| HESS J1702-420 | 17h2m44.6s | -42d4' 22'' | ~7% | ~5 | -- | ApJ 636 (2006) 777 |
| HESS J1708-410 | 17h8m14.3s | -41d4' 57'' | ~4% | ~3 | -- | ApJ 636 (2006) 777 |
| HESS J1713-381 | 17h13m58.0s | -38d11' 43'' | ~2% | ~4 | G348.7+0.3 ? | ApJ 636 (2006) 777 |
| HESS J1713-397 | 17h13m | -39d45’ | ~66% | ~15 | **RXJ 1713.7-3946, G347.3-0.5** | Nature 432 (2004) 75 |
| HESS J1745-290 | 17h45m41.3s | -29d0' 22” | ~5% | < 3 | Sgr A* / Sgr A East ? | A&A 425 (2004) L13 |
| HESS J1745-303 | 17h45m2.2s | -30d22' 14'' | ~5% | ~9 | 3EG J1744-3011 ? | ApJ 636 (2006) 777 |
| HESS J1747-281 | 17h47m23.2s | -28d9' 6” | ~2% | <1.3 | G0.9+0.1 | A&A 432 (2005) L25 |
| HESS J1804-216 | 18h4m31.6s | -21d42' 3'' | ~25% | 12 | G8.7-0.1, PSR J1803-2137 ? | Science 307 (2005) 1938 |
| HESS J1813-178 | 18h13m36.6s | -17d50' 35'' | ~6% | ~2 | G12.82-0.02, AX J1813-178 ? | Science 307 (2005) 1938 |
| HESS J1825-137 | 18h26m3.0s | -13d45' 44'' | ~17% | ~10 | PSR J1826-1334 / 3EG J1826-1302 ? | Science 307 (2005) 1938 |
| HESS J1826-148 | 18h26m15s | -14d49' 30'' | ~3% | not extended | **LS 5039** | Science 309 (2005) 746 |
| HESS J1834-087 | 18h34m46.5s | -8d45' 52'' | ~8% | ~5 | G23.3-0.3 / W41 ? | Science 307 (2005) 1938 |
| HESS J1837-069 | 18h37m37.4s | -6d56' 42'' | ~13% | ~5 | G25.5+0.0, AX J1838-0655 ? | Science 307 (2005) 1938 |
| HESS J2009-488 | 20h9m29.3s | -48d49' 19'' | ~2.5% | not extended | **PKS 2005-489** | A&A 436 (2005) L17 |
| HESS J2158-302 | 21h58m52.7s | -30d13' 18” | up to 50% | not extended | **PKS 2155-304** | * A&A 430 (2005) 865 |

# Status of the γ-astronomy field

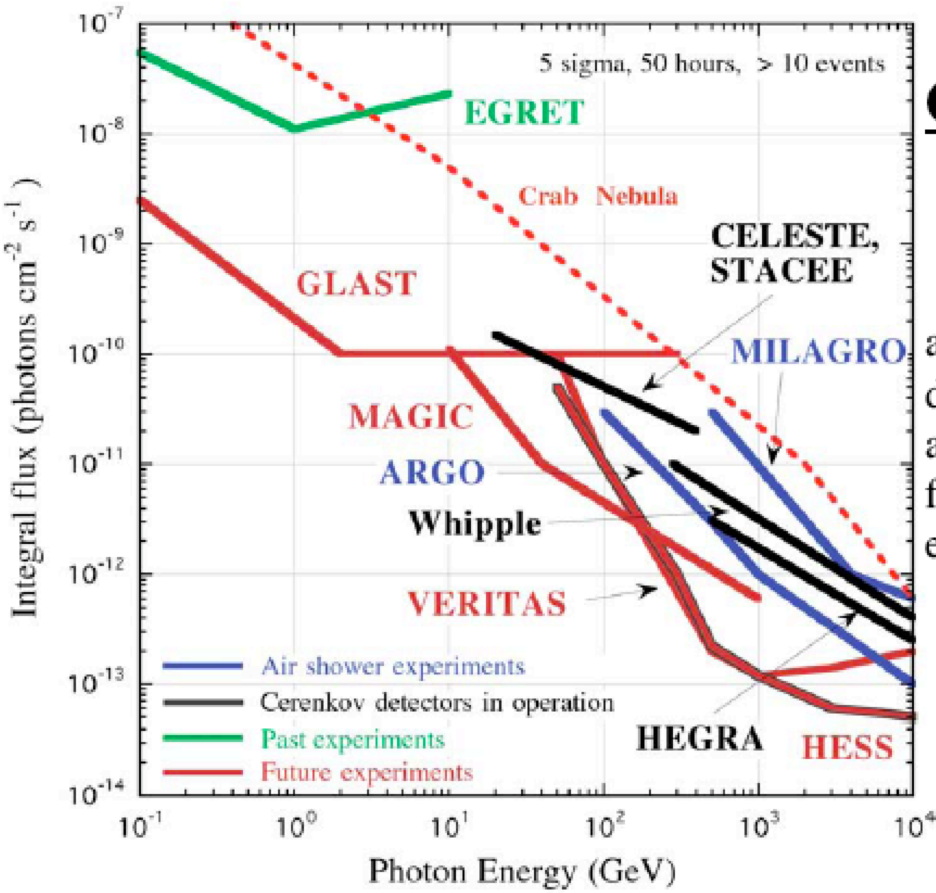


## Complementary capabilities

| | ground-based | | space-based |
|---|---|---|---|
| | ACT | EAS | Pair |
| angular resolution | good | fair | good |
| duty cycle | low | high | high |
| area | large | large | small |
| field of view | small | large | large+can reorient |
| energy resolution | good | fair | good, w/ smaller systematic uncertainties |

The next-generation ground-based and space-based experiments are well matched.

# Previous missions: BATSE and EGRET on CGRO

**The high energy gamma ray detector on the Compton Gamma Ray Observatory (20 MeV - ~20 GeV)**

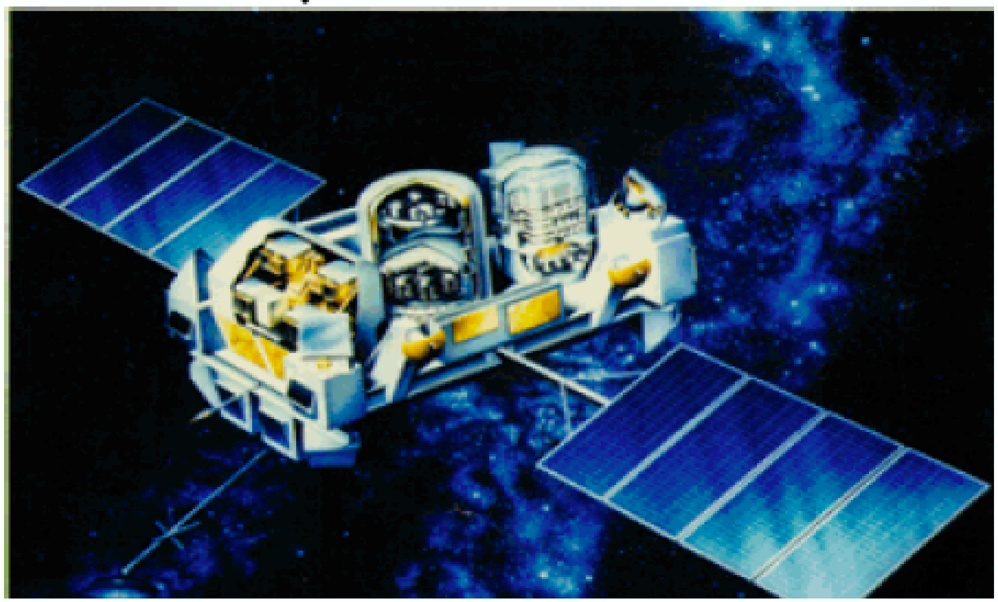

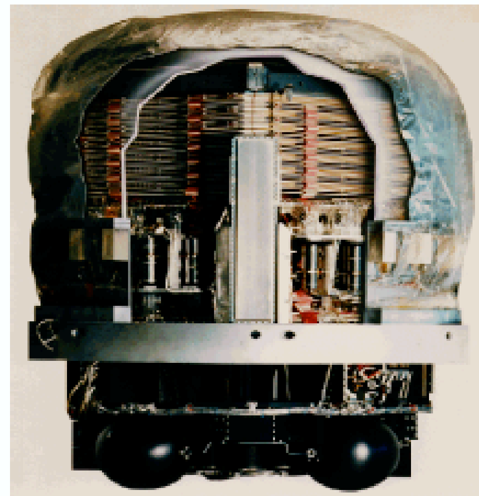

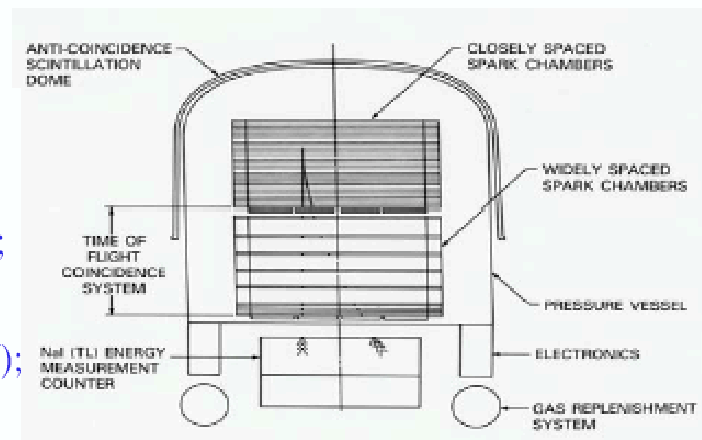


EGRET (1990's) established field:

- increased number of ID'd sources by large factor;
- broadband measurements covering energy range ~20 MeV - ~20 GeV;
- discovered many still-unidentified sources;
- discovered surprisingly large number of Active Galactic Nuclei (AGN);
- discovered multi-GeV emissions from gamma-ray bursts (GRBs);
- discovered GeV emissions from the sun

# GLAST: Gamma Ray Large Area Space Telescope

Launch in late 2007.

- Main instrument: LAT (Large Area Telescope) sensitive to gamma rays between 20 MeV-300 GeV
- GBM (GLAST Burst Monitor) X-rays and $\gamma$-rays between 5 keV-25MeV

Mission duration > 5 yrs

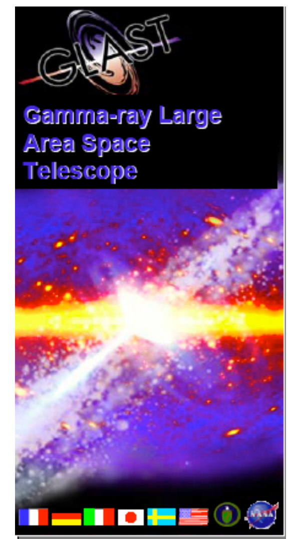


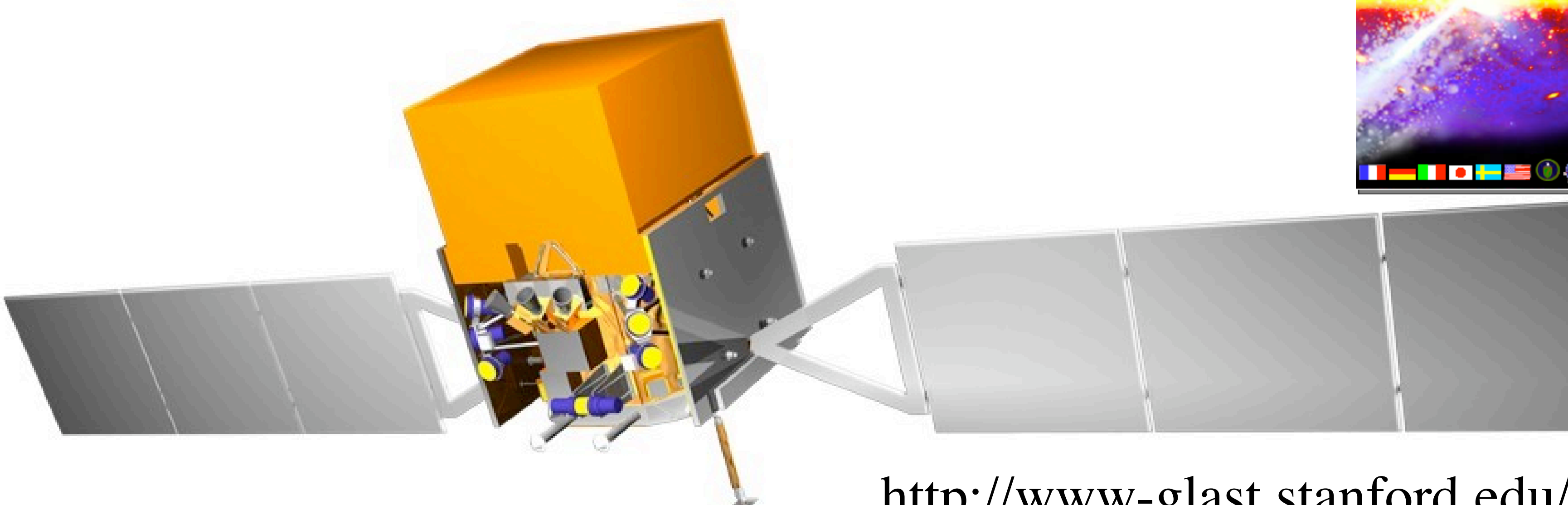

http://www-glast.stanford.edu/

# Advancing wih GLAST

- Huge FOV (~20% of sky)
- Broadband (4 decades in energy, including unexplored region > 10 GeV)
- Unprecedented PSF for gamma rays (factor > 3 better than EGRET for E>1 GeV)
- Large effective area (factor > 4 better than EGRET)
- **Results in factor > 30-100 improvement in sensitivity**

# EGRET/GLAST

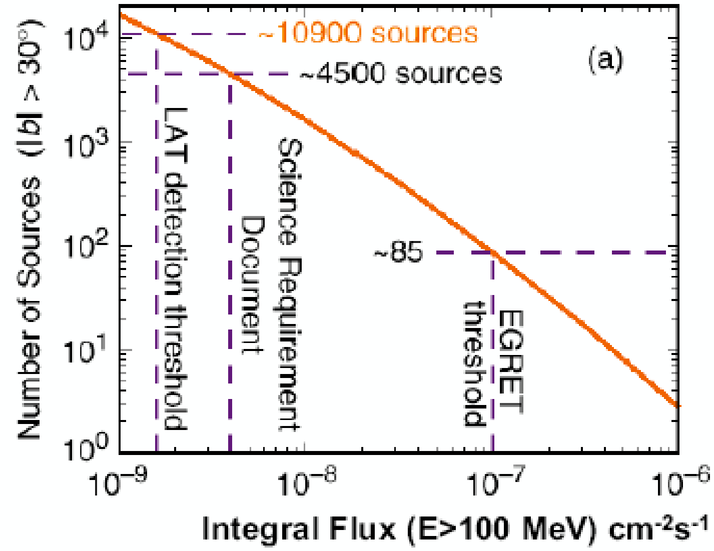


172 of the 271 sources in the EGRET 3rd catalog are "unidentified"

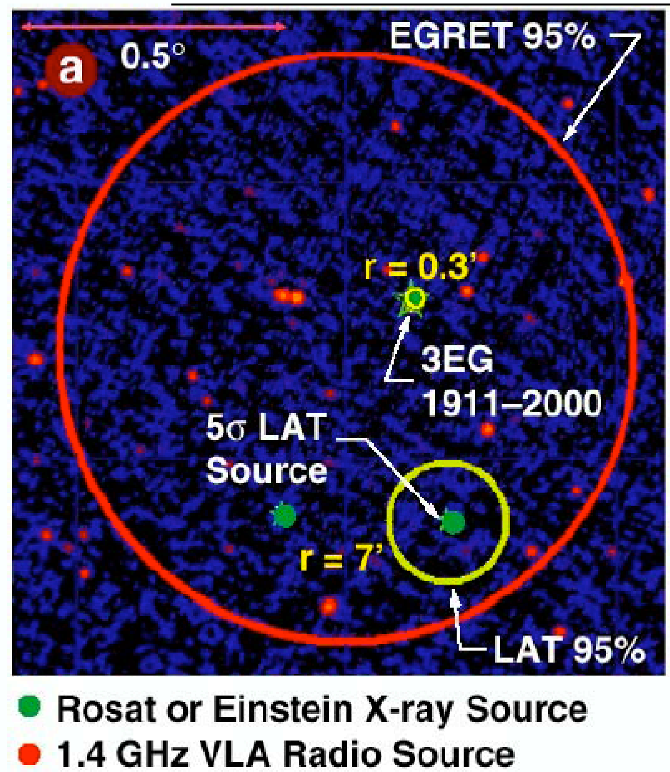


EGRET source position error circles are ~0.5°, resulting in counterpart confusion.

GLAST will provide much more accurate positions, with ~30 arcsec - ~5 arcmin localizations, depending on brightness.

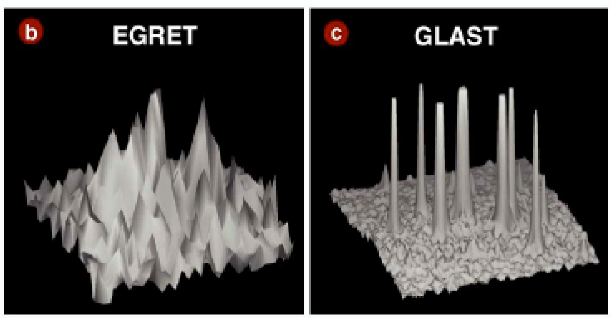


Cygnus region (15x15 deg)

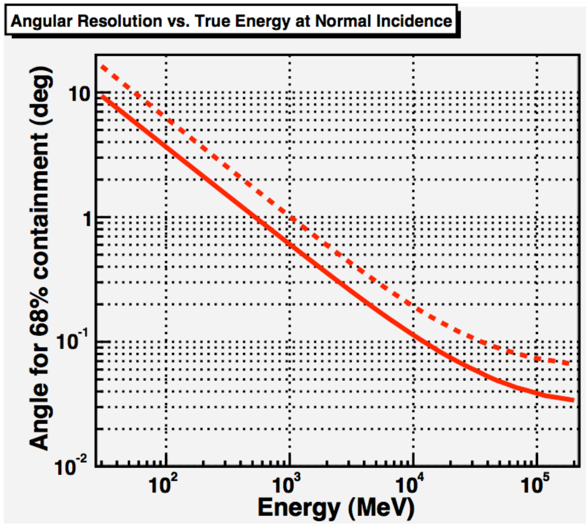


# Definitions

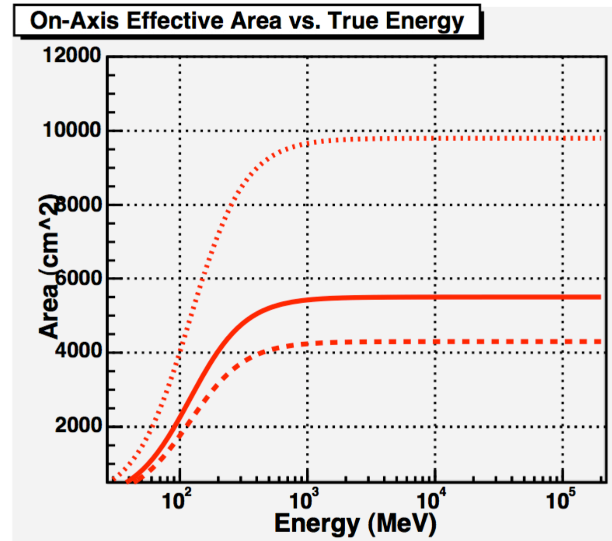


## Effective area

(total geometric acceptance) • (conversion probability) • (all detector and reconstruction efficiencies). Real rate of detecting a signal is (flux) • $A_{eff}$

## Point Spread Function (PSF)

Angular resolution of instrument, after all detector and reconstruction algorith effects. The 2-dimensional 68% containment is the equivalent of ~1.5σ (1-dimensional error) if purely Gaussian response. The non-Gaussian tail is characterized by the 95% containment, which would be 1.6 times the 68% containment for a perfect Gaussian response.

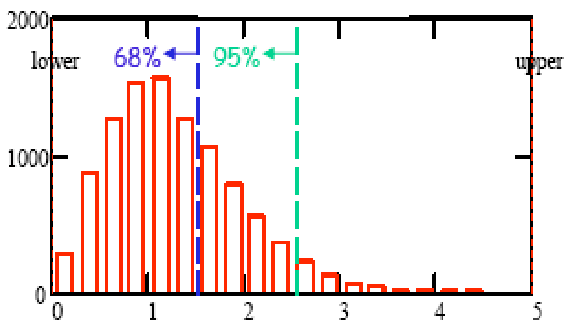


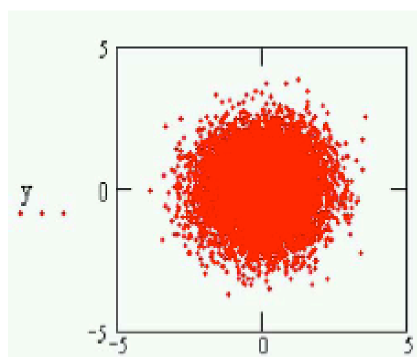


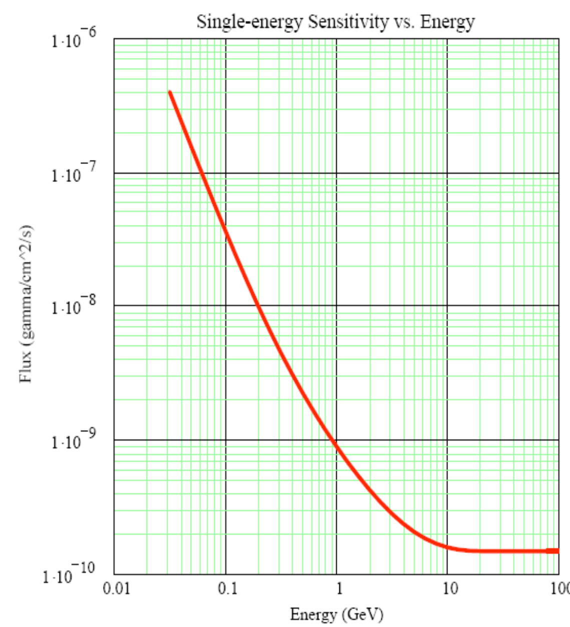

# Scientific requirements

| Parameter | SRD Value |
|---|---|
| Peak Effective Area (in range 1-10 GeV) | >8000 $cm^2$ |
| Energy Resolution 100 MeV on-axis | <10% |
| Energy Resolution 10 GeV on-axis | <10% |
| Energy Resolution 10-300 GeV on-axis | <20% |
| Energy Resolution 10-300 GeV off-axis (>60$^o$) | <6% |
| PSF 68% 100 MeV on-axis | <3.5° |
| PSF 68% 10 GeV on-axis | <0.15° |
| PSF 95/68 ratio | <3 |
| PSF 55$^o$/normal ratio | <1.7 |
| Field of View | >2sr |
| Background rejection (E>100 MeV) | <10% diffuse |
| Point Source Sensitivity(>100MeV) | <6x10$^{-9}$ $cm^{-2}s^{-1}$ |
| Source Location Determination | <0.5 arcmin |
| GRB localization | <10 arcmin |

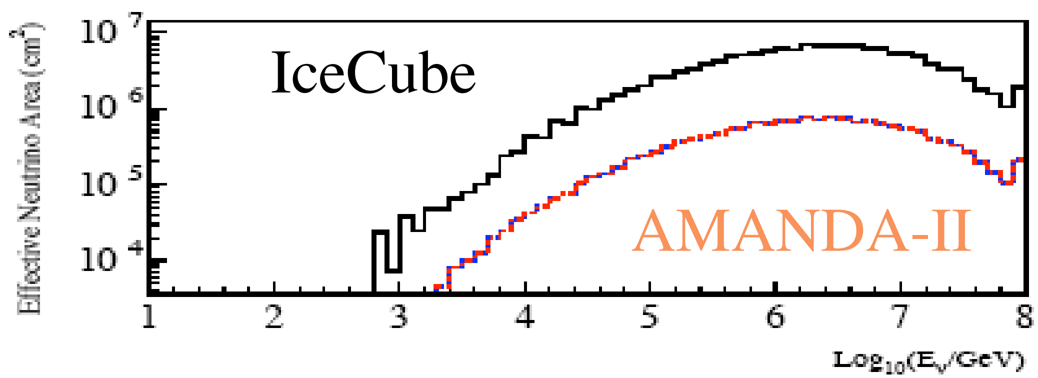

# Experimental technique

- Measure direction, energy and arrival time of high energy photons (20 MeV-300 GeV)
- Dominated by pair production: clear signature for background rejection
- Background of CR is about $10^4$ larger than $\gamma$ signal

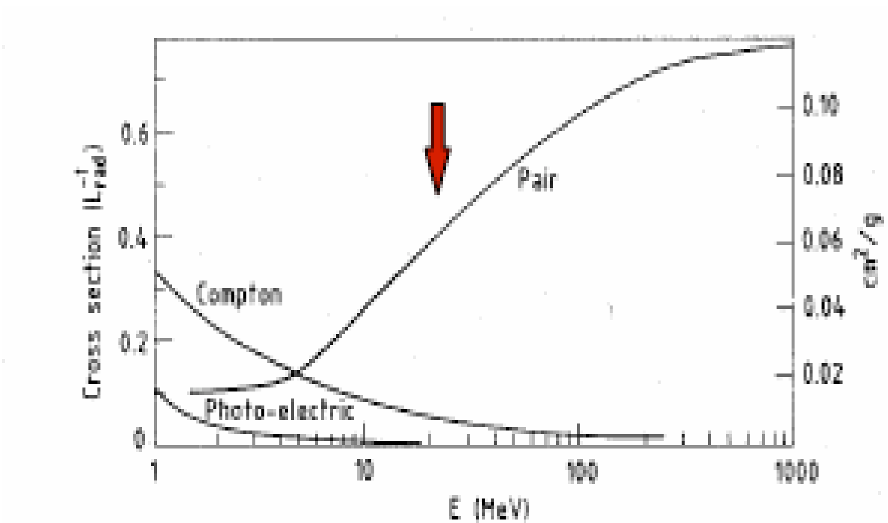


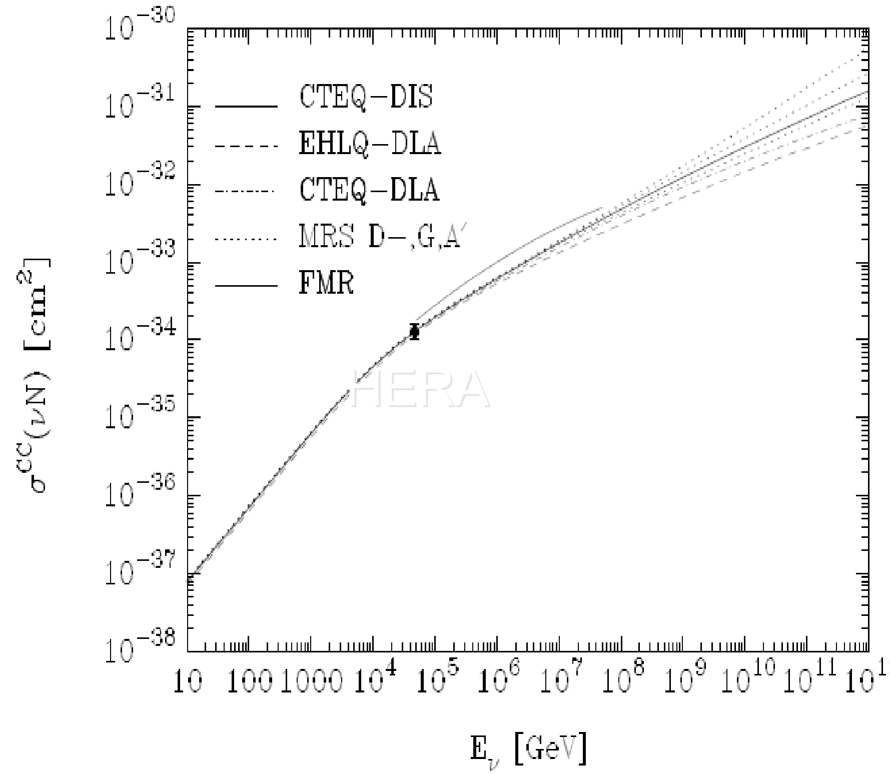


**Neutrini are much harder to detect than photons!**

# LAT: the main detector

Pair conversion detector built with:

- plastic anticoincidence shield,
- segmented CsI em calorimeter
- the largest Si strip tracker with slabs of tungsten converter ever built. 4 x 4 identical towers surrounded by an anticoincidence (ACD) to identify charged CRs

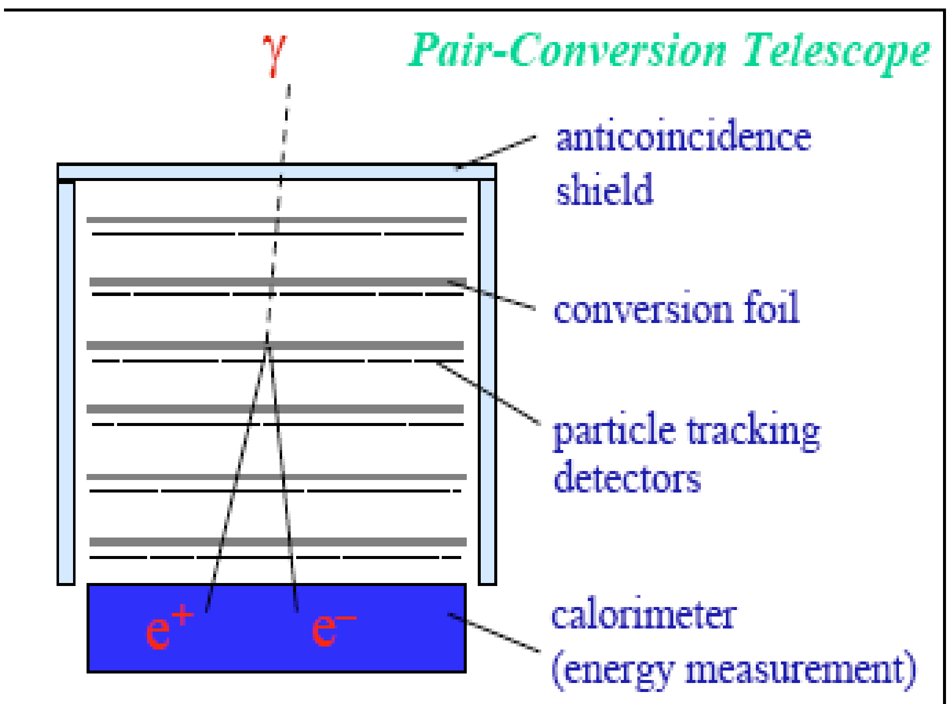


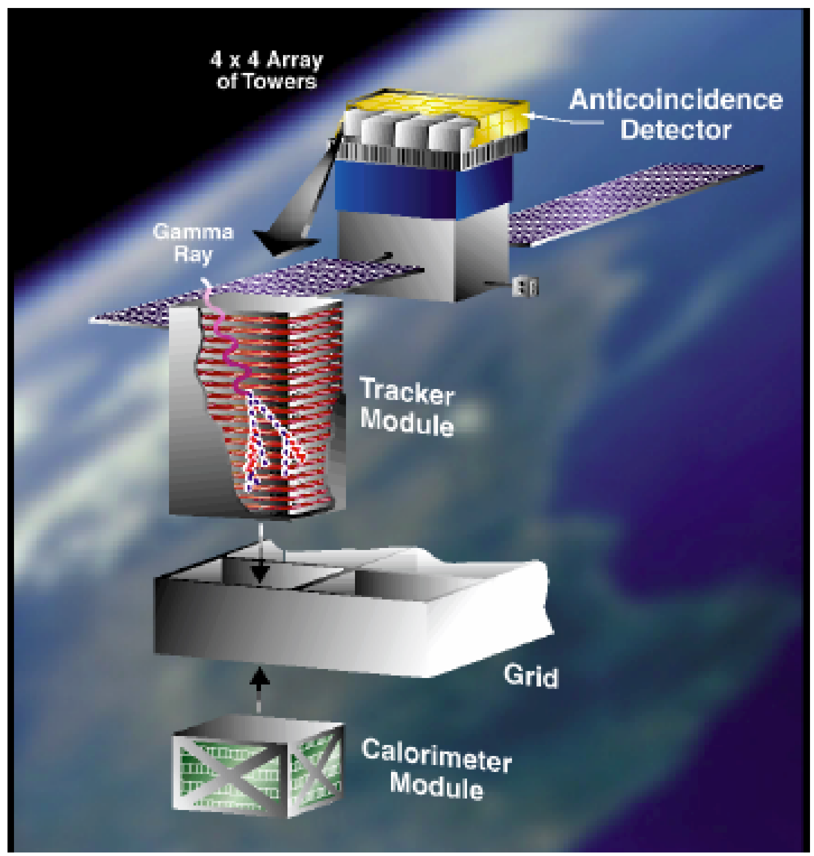

# Instrument Design

- limitations on angular resolution (PSF)
  - **low E: multiple scattering => many thin layers**
  - **high E: hit precision & lever arm**

Effective area and PSF requirements drive the converter thicknesses and layout. PSF requirements also drive the sensor performance, layer spacings, and drive the design of the mechanical supports.

Background rejection requirements drive the ACD design (and influence the calorimeter and tracker layouts).

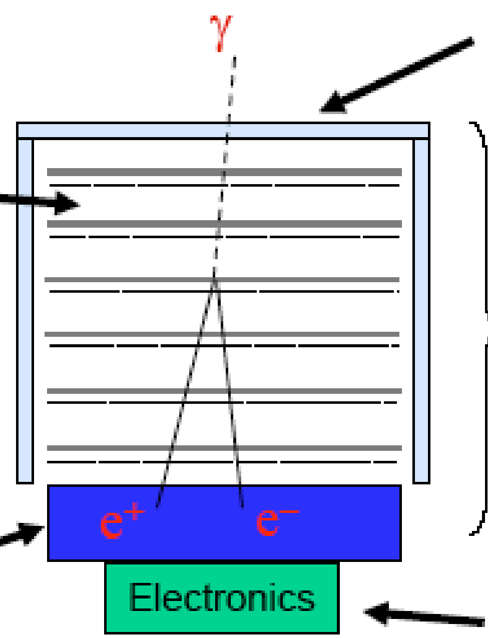


Field of view sets the aspect ratio (height/width)

Energy range and energy resolution requirements bound the thickness of calorimeter

Time accuracy provided by electronics and intrinsic resolution of the sensors.

On-board transient detection requirements, and on-board background rejection to meet telemetry requirements, are relevant to the electronics, processing, flight software, and trigger design.

Instrument life has an impact on detector technology choices.
Derived requirements (source location determination and point source sensitivity) are a result of the overall system performance.

# GBM

## 12 Sodium Iodide (NaI) Scintillation Detectors

### Characteristics

- 5-inch diameter, 0.5-inch thick
- One 5-inch diameter PMT per Det.
- Placement to maximize FoV
- Thin beryllium entrance window
- Energy range: ~5 keV to 1 MeV

### Major Purposes

- Provide low-energy spectral coverage in the typical GRB energy regime over a wide FoV
- Provide rough burst locations over a wide FoV

## 2 Bismuth Germanate (BGO) Scintillation Detectors

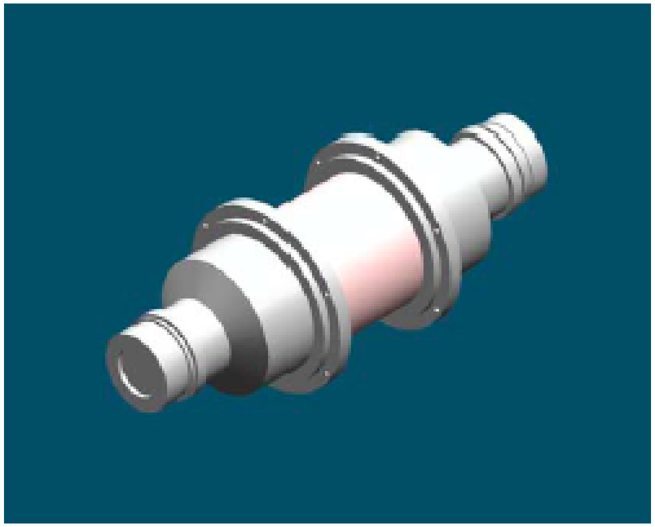

### Characteristics

- 5-inch diameter, 5-inch thick
- High-Z, high-density
- Two 5-inch diameter PMTs per Det.
- Energy range: ~150 keV to 30 MeV

### Major Purpose

- Provide high-energy spectral coverage to overlap LAT range over a wide FoV

# Constraints to Design

•Mass < 3000 kg (restricts calorimeter depth)

•Lateral dimensions < 1.8 m (restricts the geometric area)

•Power < 650 W (restricts number of readout channels and onboard CPU)

•Telemetry bandwidth < 300 kpbps (kbits per s) (sets the required level of onboard background rejection and data volume per event)

•Launch loads and other environmental constraints

# Sensitivity to GRBs

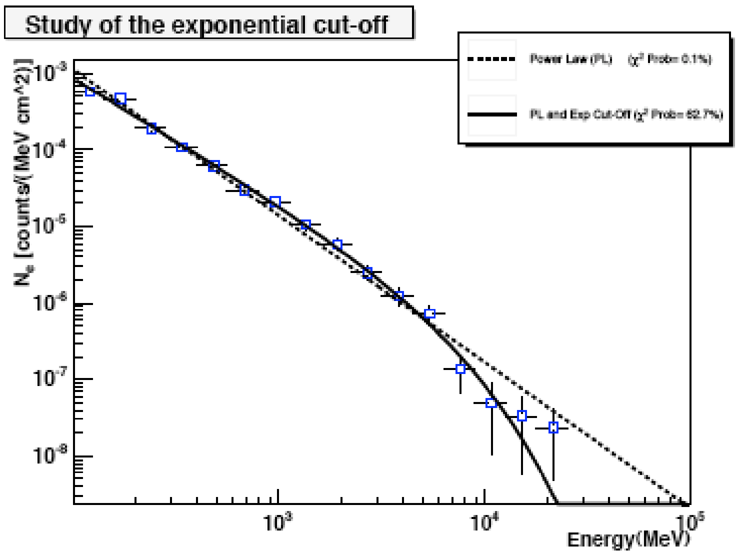


Reconstruction of spectra:; real cut-off at 4.5 GeV, reconstructed at 5.5 ± 1.5 GeV

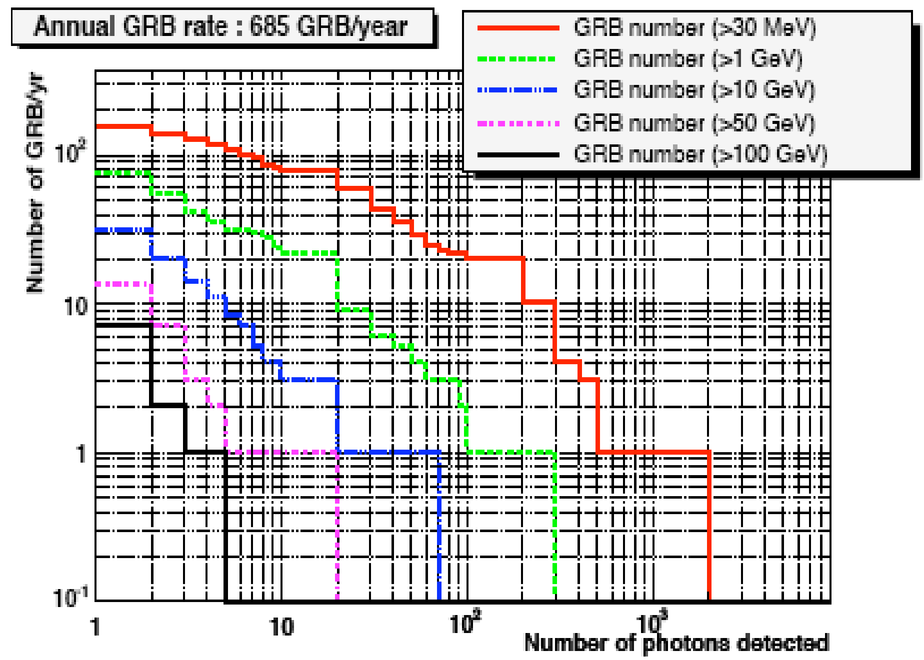


**FIGURE 3.** Model-dependent LAT GRB sensitivity assuming a mean burst rate of 650 bursts/yr, including the effect of the EBL absorption. Different curves refer to different energy thresholds.

# Alerts for GRBs

For 5 yrs GLAST will scan uniformly the full sky in 3 hrs (scanning mode)

GBM and LAT will trigger independently on GRBs, GBM on a rapid increase of counts and LAT considering spatial and temporal clustering of counts

GBM will detect 200 bursts/yr of which more than 60 will fall in LAT FoV
Alerts will be sent to ground with a satellite communication system within 10 s
The initial on-board GBM localization accuracy is about 15 degrees within 1.8 s that can be used by LAT. Updates come later and reduce the GBM localization error box up to about 5 degrees for a bright burst while the **LAT can provide accuracy up to tens of arcminutes (1 arcmin = 0.01666 deg)** depending on burst intensity

About 20/yr SWIFT detected GRBs will be in LAT FoV